

Investigation of binary Co_2X ($\text{X} = \text{In}, \text{Si}, \text{Sb}, \text{Sn}, \text{Ga}$) half-Heusler alloys

Adewumi Isaac POPOOLA*

Department of Physics, Federal University of Technology, Akure, Nigeria

Received: 05.09.2016

Accepted/Published Online: 20.01.2017

Final Version: 18.04.2017

Abstract: The electronic structure and mechanical properties of some cobalt-based binary half-Heusler alloys Co_2X ($\text{X} = \text{In}, \text{Si}, \text{Sb}, \text{Sn}, \text{Ga}$) have been investigated using the density functional theory approach. The site preference by cobalt and X is similar to the traditional half-Heusler structure. The results showed that Co_2Si is not a half-metal but rather an n-type degenerate semiconductor. The compounds Co_2Ga , Co_2Sb , and Co_2Sn are thermodynamically unstable and Co_2In is elastically unstable. With much care given to the lattice size, half metallicity is readily predicted in Co_2In , Co_2Ga , Co_2Sn , and Co_2Sb . All the compounds showed directional bonding and they should exhibit high strength. The trend is that the low valence main group elements are likely to form half metals more readily in a binary half-Heusler alloy than the high valence main group elements.

Key words: Cobalt, half-Heusler, spintronic, density of states, n-type degenerate

1. Introduction

Heusler alloys have attracted much attention for more than a century since their discovery by Fritz Heusler, a German mining engineer and chemist. The interest in Heusler alloys is likely to continue for another century for two main reasons: their interesting diverse magnetic phenomena [1–4] and their flexible electronic structure, which could serve as a good foundation upon which other materials of optimum functionalities can be realized [5,6]. Heusler alloys hold great potential for spintronic device applications, thermoelectrics, and solar cells. Heusler alloys were first discovered in the form X_2YZ , which crystallizes in the L2_1 structure with four fcc sublattices (Figure 1). Two of the four sublattices are occupied by the same type of X atoms, while Y and Z occupy the remaining two. Thereafter, other Heusler alloys of the C1_b structure were discovered. The chemical formula for this second group is XYZ, where one sublattice remains unoccupied. The latter compounds are often called half-Heusler alloys, while the L2_1 compounds are referred to as full Heusler alloys. In Heusler alloys, X and Y are transition *d*-elements while Z is a III, IV, or V group element. Investigations have shown that the conventional stable structure for the half-Heusler alloys is when X and Y atoms are located at the A(0,0,0) and B(1/4,1/4,1/4) Wyckoff positions and the Z atom is located at the D(3/4,3/4,3/4) position, respectively, leaving the C(1/2,1/2,1/2) position unoccupied [7–10]. For spintronic applications, the half-metallic character is important. In the half-Heusler structure, the first alloy described in light of this concept was NiMnSb. It was discovered using the first-principle calculation based on density functional theory [11]. Since then, other compounds like PtMnSb, NiCrZ, and MnCrSb [12–14] have been described. Recently, Jianqiang et al. reported half-metallicity in the binary alloys Fe_2Z ($\text{Z} = \text{In}, \text{Sn}, \text{Sb}, \text{and As}$) with a half-Heusler structure [15]. Apart

*Correspondence: ispopoola71@gmail.com

from the Heusler family of alloys, other compounds that have shown half-metallicity include CrO_2 [16], Fe_3O_4 [17], oxide perovskites [18], and double perovskites [19]. In the case of the ternary (XYZ) half-Heusler alloys, formation of half-metallicity is easily influenced when X is a high valence 3-d atom and Y a low valence 3-d atom [4]. Unlike the ternary alloy, the X and Y atoms in binary half-Heusler alloys are the same. Therefore, the aim of the present work is to study the binary half-Heusler alloys of the form Co_2X ($\text{X} = \text{In}, \text{Si}, \text{Sb}, \text{Sn}, \text{Ga}$). Investigating such binary half-Heusler alloys may help us to gain insights on the electronic structure, bonding, and potential application of these binary half-Heusler compounds. In this light, the site preference, electronic structure, and elastic properties of cobalt-based binary half-Heusler alloys Co_2X ($\text{X} = \text{In}, \text{Si}, \text{Sb}, \text{Sn}, \text{Ga}$) are studied.

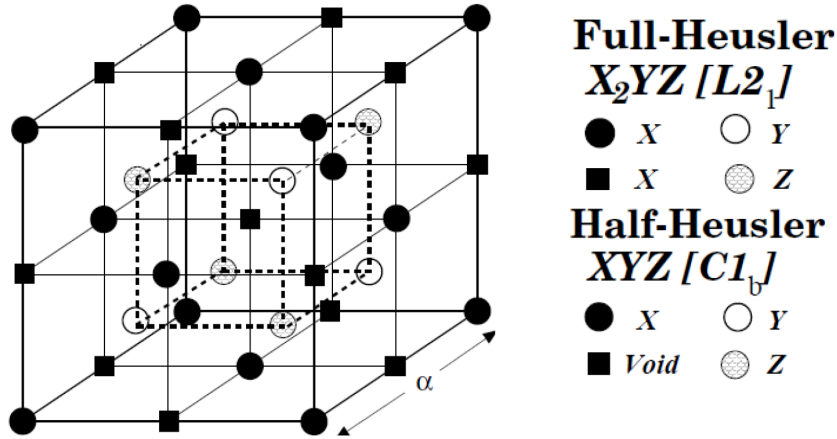


Figure 1. $C1_b$ and $L2_1$ structures adapted by the half- and full-Heusler alloys. In the case of the ternary XYZ half-Heusler: X at (0 0 0), Y at (1/4, 1/4, 1/4), a vacant site at (1/2, 1/2, 1/2), and Z at (3/4, 3/4, 3/4) in Wyckoff coordinates. For the full-Heusler alloys (X_2YZ), the vacant site is occupied by an X atom.

2. Computational method

All calculations were based on density functional theory [20,21] as implemented in the QUANTUM ESPRESSO code [22]. The electronic exchange-correlation functional was treated with the generalized gradient approximation (GGA) of Perdew et al. [23]. Co ($3d^7 4s^2$), Ga ($4s^2 4p^1$), In ($4d^{10} 5s^2 5p^1$), Si ($3s^2 3p^2$), Sn ($5s^2 5p^2$), and Sb ($5s^2 5p^3$) respectively were treated as valence by the pseudopotentials. The Kohn–Sham orbitals were described with plane-wave basis sets. The electronic wave functions were truncated with energy-cutoff of 50 Ry. The Marzari–Vanderbilt smearing size was fixed at 0.04 Ry. The Monkhorst–Pack scheme [24] was used for the Brillouin zone integration with a shifted mesh of $10 \times 10 \times 10$ for the self-consistent field calculations.

3. Results and discussion

In a traditional half-Heusler compound, the $C(1/2, 1/2, 1/2)$ site is vacant. For this reason, the first task was to investigate the site preference of cobalt in the half-Heusler-type structure.

Two kinds of site occupation were considered. The first was the normal half-Heusler structure where Co atoms enter the $A(0,0,0)$ and $B(1/4,1/4,1/4)$ sites, while the other had the two Co atoms entering the $A(0,0,0)$ and $C(1/2, 1/2, 1/2)$ sites. Each configuration was optimized for three different cases: nonmagnetic, ferromagnetic, and antiferromagnetic. The equilibrium lattice parameter and energy for each composition was

determined by a fit to the Birch–Murnaghan equation of state. The equilibrium lattice energy obtained showed that the structure with cobalt (Co) entering the A and C sites is higher in energy compared with Co entering the A and B sites. This indicates that Co_2X ($\text{X} = \text{In}, \text{Si}, \text{Sb}, \text{Sn}, \text{Ga}$) compounds would also prefer to crystallize in the traditional half-Heusler structure.

3.1. Thermodynamic stability

By conventional means, it should be possible to make any substance that is thermodynamically stable. In ab initio studies, the energy of formation (ΔE^\ominus) is traditionally used to study the thermodynamic stability of a material. In the case of Co_2X compounds, the energy of formation is the energy of Co_2X relative to pure Co and isolated X ($\text{X} = \text{In}, \text{Si}, \text{Sb}, \text{Sn}, \text{Ga}$) atoms in their equilibrium crystal structures and it was evaluated according to Eq. (1):

$$\Delta E^\ominus(\text{Co}_2\text{X}) = \frac{1}{3}E_{\text{Co}_2\text{X}}^\ominus - \left[\frac{2}{3}E_{\text{Co}}^\Phi + \frac{1}{3}E_{\text{X}}^\psi \right] , \quad (1)$$

where $\Delta E_{\text{Co}_2\text{X}}^\ominus$ is the total energy of Co_2X with \ominus structure, E_{Co}^Φ is the total energy per atom of Co with Φ structure, and E_{X}^ψ is the total energy per atom of X with ψ structure. A negative heat of formation energy would indicate a thermodynamically stable material, while a positive value indicates an unstable or metastable material. Listed in Table 1 are the lattice parameter (a_0), the formation energy (ΔE^\ominus), the equation of states equilibrium energy (E_0), and magnetic moments (M_t) for the Co_2X ($\text{X} = \text{In}, \text{Si}, \text{Sb}, \text{Sn}, \text{Ga}$) compounds. Based on the E_0 result, all the alloys are ferromagnets. The ΔE^\ominus results show that Co_2Si and Co_2In are stable while Co_2Sn , Co_2Sb , and Co_2Ga are predicted to be thermodynamically unstable.

Table 1. Calculated equilibrium lattice constants a_0 , energy E_0 , formation energy (ΔE^\ominus), and total magnetic moments M_t of Co_2X ($\text{X} = \text{In}, \text{Si}, \text{Sb}, \text{Sn}, \text{Ga}$). NM: Nonmagnetic state, FM: ferromagnetic, and AFM: antiferromagnetic state.

| Alloy | States | a_0 (Å) | E_0 (Ry) | ΔE^\ominus (Ry) | M_t (μ_B/atom) |
|------------------------|--------|-----------|------------|-------------------------|-------------------------------|
| Co_2In | NM | 5.74131 | -285.34732 | - | - |
| | FM | 5.83229 | -285.37515 | -101.148 | 1.1 |
| | AFM | 5.75990 | -285.34832 | - | - |
| Co_2Sn | NM | 5.72536 | -155.74840 | - | - |
| | FM | 5.43275 | -153.19352 | 7.277 | 0.33 |
| | AFM | 5.72536 | -155.74840 | - | - |
| Co_2Sb | NM | 5.71782 | -159.85712 | - | - |
| | FM | 5.77059 | -159.87610 | 213.897 | 0.44 |
| | AFM | 5.43275 | -153.19352 | - | - |
| Co_2Si | NM | 5.33027 | -156.70184 | - | - |
| | FM | 5.36531 | -156.72170 | -98.328 | 0.33 |
| | AFM | 5.30404 | -156.70216 | - | - |
| Co_2Ga | NM | 5.4302 | -153.17977 | - | - |
| | FM | 5.4891 | -153.19379 | 866.833 | 1.1 |
| | AFM | 5.4821 | -153.19377 | - | - |

3.2. Density of states

Many physical properties of a material can be evaluated from its electronic structure. The density of states (DoS), which describes the states per interval of energy available for electron occupation, can be used to

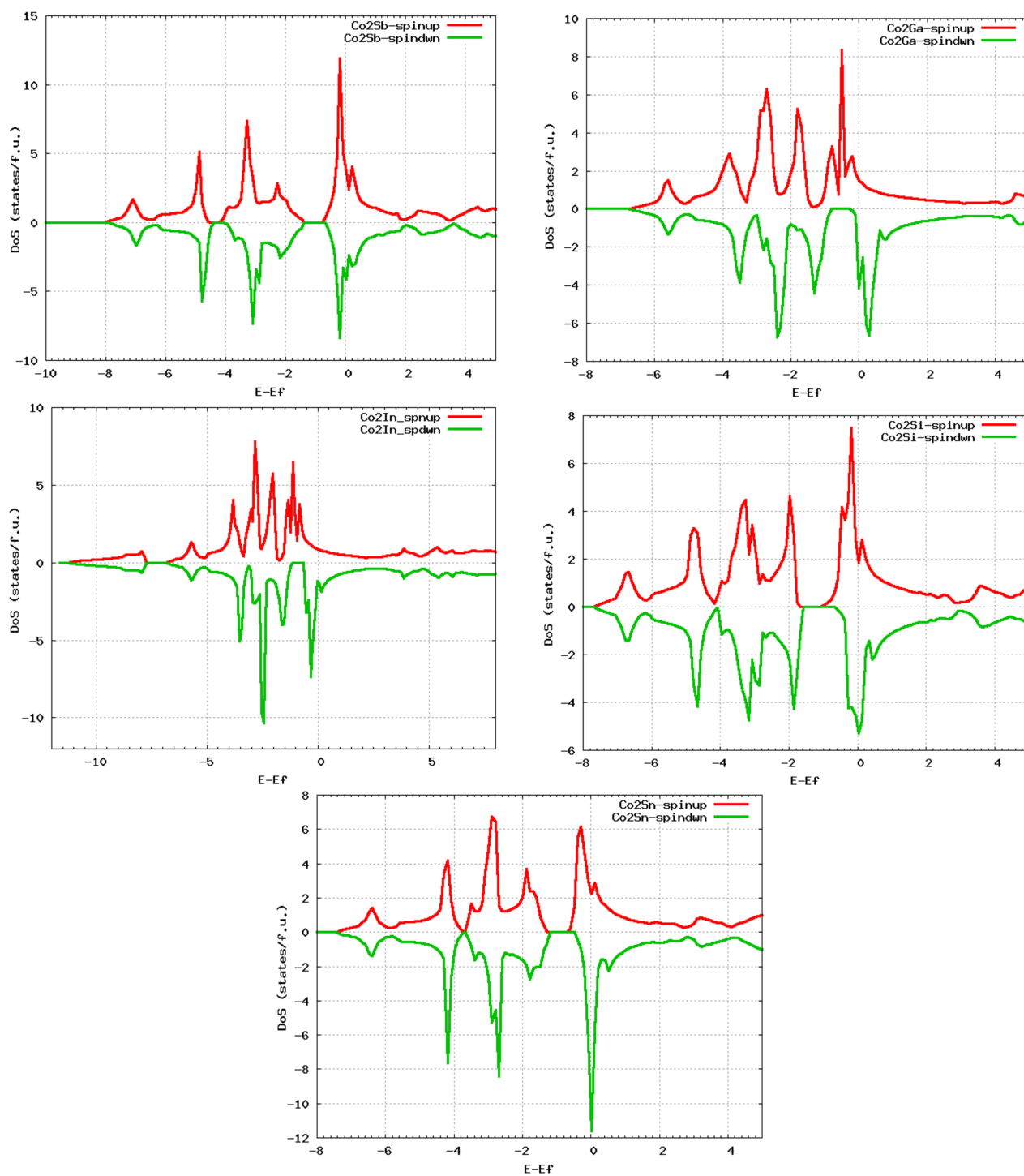


Figure 2. a) Density of states plots for Co_2Sb . b) Density of states plots for Co_2Ga . c) Density of states plots for Co_2In . d) Density of states plots for Co_2Si . e) Density of states plots for Co_2Sn .

understand phenomena like phase stability, melting, etc. The DoS for the Co_2X compounds is given in Figures 2a–2e. First, it is noted that all the plots show exchange splitting (the DoS at the Fermi level (E_F) for the spin-down is higher than for the spin-up), which further confirms that all the Co_2X compounds are ferromagnetic.

We see from Figures 2a through 2e that the ferromagnetism would be highest in Co_2Sn , followed by Co_2Si , then Co_2Ga and Co_2In , and least in Co_2Sb . Half metallicity is predicted in Co_2Ga , Co_2In , Co_2Si , and Co_2Sn and not in Co_2Sb . While the spin-up at and around the Fermi level (E_F) shows metallic character, there are gaps in the spin-down bands below the Fermi level for Co_2Ga , Co_2In , Co_2Si , and Co_2Sn . In materials for spintronic applications, the spin-up band should show a metallic character, and in the spin-down band, a semiconducting character should be seen. The deviation of the DoS plots from these ideals can be attributed to the used exchange-correlation functional (the GGA), which is known to overpredict structural parameters such as the lattice parameter. For half-metals, variations (compression or expansion) in the lattice parameter would impact the position of E_F [10].

3.3. Band structure

For technological applications, the suitability or otherwise of a material can be affected by the type of energy gap existing in the material. To evaluate the type of gap existing in the spin-down band of the Co_2X materials, a detailed calculation of their band structure along high symmetry points was performed and these results are presented in Figure 3a–3e.

First, it can be predicted from the plots that Co_2Si , Co_2Sb , and Co_2Sn are direct gap materials, while Co_2Ga and Co_2In are indirect gap materials. For Co_2Ga and Co_2In , the Fermi level (E_F) is located at the gap. The gap narrows due to the bottom of the conduction band overlapping with E_F at X. This can be attributed to volume expansion. If Co_2Ga and Co_2In are allowed to contract, the tendency is that the Fermi level would move in the direction of the valence band.

Thankfully, materials for spintronic applications are prepared as thin films, and since thin films are grown on a substrate, it is possible to influence the lattice constant of the grown thin film by adjusting the lattice of the substrate used. The band structures of Co_2Si , Co_2Sb , and Co_2Sn are quite similar in that the Fermi level is located above the bandgap. At ground state, many extra electrons are found in the conduction band. Obviously, the compounds are predicted to be degenerate n-type semiconductors and not metals. The implication is that these materials could act as transparent conductors with potential for thermoelectric applications.

3.4. Mechanical properties

For engineering applications, the mechanical property of a material is important. The elastic constants, which determine the response of a material to applied stress, are a good starting point in understanding properties like phase stability, hardness, toughness, melting points, etc. Using the Catti method [25,26], the three elastic constants c_{11} , c_{12} , and c_{44} for all the compounds were calculated. From the elastic constants, the bulk modulus (B), shear modulus (E), Young modulus (Y), Poisson ratio (ν), and Debye temperature (Θ_D) were calculated. The elastic moduli were calculated with the Hill [27] averaging methods. For the purpose of the present work, the expression [28,29] used to evaluate the Debye temperature is written as:

$$\Theta_D = C \left(\frac{aG_B}{M} \right)^{\frac{1}{n}}, \quad (2)$$

$$G_B = [c_{44}(c_{11} - c_{12}(c_{11} + c_{12} + 2c_{44}))]^{\frac{1}{3}}, \quad (3)$$

$$C = 3.89 \times 10^{11} s^{-\frac{1}{6}} \frac{\hbar}{k_B}, \quad (4)$$

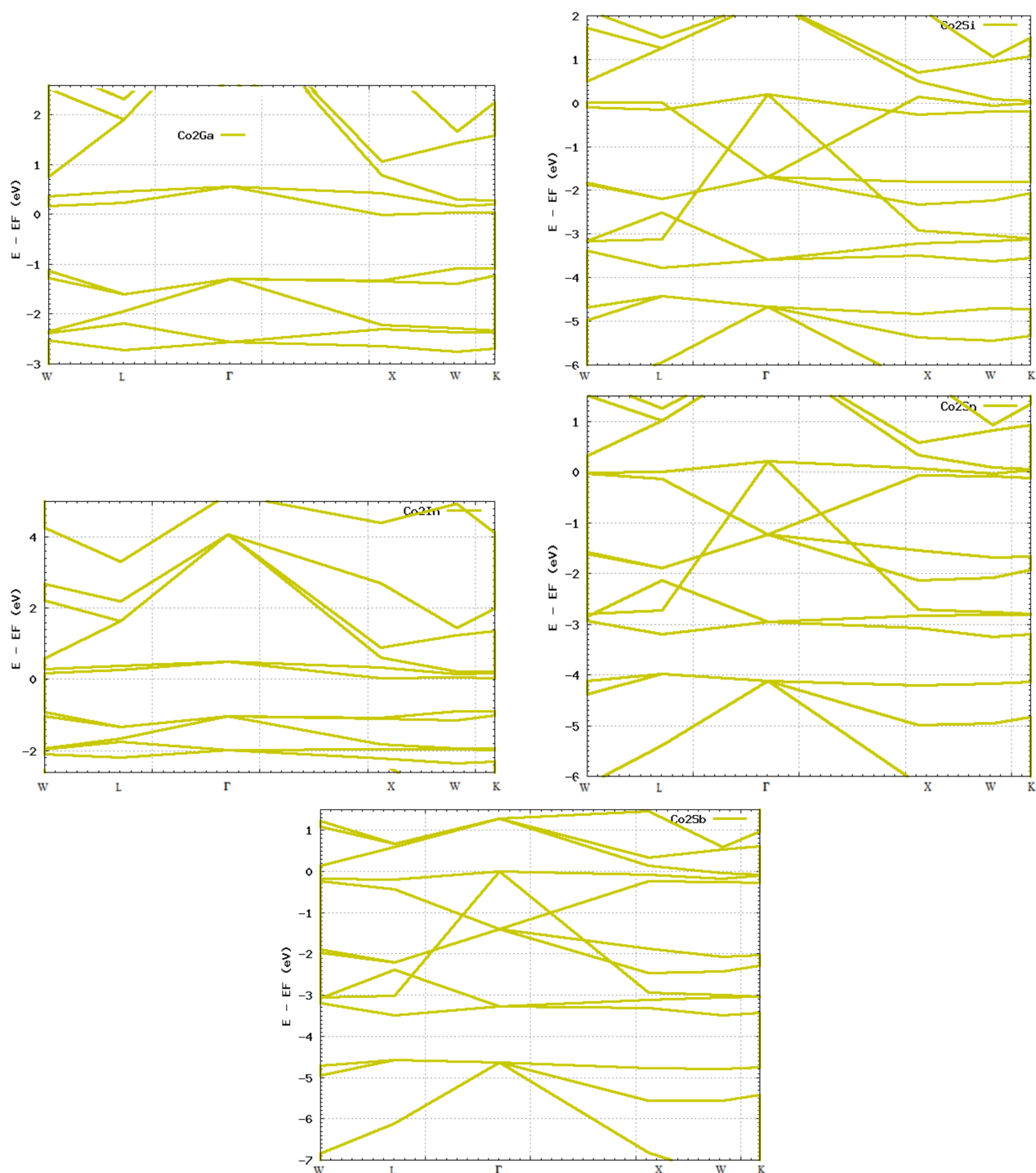


Figure 3. Band structure plots along line of high symmetry for Co₂Ga. b) Band structure plots along line of high symmetry for Co₂Si. c) Band structure plots along line of high symmetry for Co₂In. d) Band structure plots along line of high symmetry for Co₂Sn. e) Band structure plots along line of high symmetry for Co₂Sb.

where $n = 2$, a is the lattice constant, M is the atomic weight (in compounds, the average of the two species), and s is the number of atoms per formula unit. The mechanical stability (MS) for each compound was tested

according to the stability criteria for cubic structures, which are:

$$c_{11} - c_{12} > 0; c_{11} - 2c_{12} > 0; c_{11} > 0; c_{44} > 0. \quad (5)$$

The results are given in Table 2.

Table 2. Calculated elastic constants (c_{11} , c_{12} , c_{44}), moduli (B, G, E), Poisson ratio (ν), Debye temperature (Θ_D), and mechanical stability in Co_2X (X = Sn, In, Ga, Sb, Si) compounds. All elastic constants and moduli are in GPa.

| Compd. | c_{11} | c_{12} | c_{44} | B | G | E | ν | Θ_D | MS |
|------------------------|----------|----------|----------|--------|-------|-------|-------|------------|----------|
| Co_2Sn | 167.80 | 93.37 | 22.44 | 118.18 | 14.05 | 40.54 | 0.448 | 24.36 | Stable |
| Co_2In | 135.60 | 82.09 | -4.78 | 99.93 | 2.26 | 6.74 | 0.489 | - | Unstable |
| Co_2Ga | 166.65 | 109.32 | 29.30 | 128.43 | 11.46 | 33.40 | 0.457 | 27.94 | Stable |
| Co_2Sb | 165.29 | 91.52 | 36.11 | 116.11 | 14.75 | 42.46 | 0.439 | 26.48 | Stable |
| Co_2Si | 203.42 | 126.52 | 50.82 | 152.15 | 14.96 | 43.45 | 0.452 | 36.49 | Stable |

From the results in Table 2, Co_2In is mechanically unstable, while other compounds are predicted to be stable. The c_{44} value of Co_2In is negative and this contravenes one of the mechanical stability criteria. Based on the shear modulus values, the hardest compound is predicted to be Co_2Si ($G = 14.96$ GPa) and the least hard material is Co_2Ga ($G = 11.46$ GPa) since Co_2In is mechanically unstable. Using the Pugh criteria [30], a material is considered ductile if its Poisson ratio is equal to or greater than 0.33. Otherwise, it is brittle.

According to the Poisson ratio values in Table 2, all the compounds are predicted to be ductile. However, the ductility is predicted to be in the order of $\text{Co}_2\text{Ga} > \text{Co}_2\text{Si} > \text{Co}_2\text{Sn} > \text{Co}_2\text{Sb}$. From the Debye temperature results, stiffness is predicted in the compounds in the order of $\text{Co}_2\text{Si} > \text{Co}_2\text{Ga} > \text{Co}_2\text{Sb} > \text{Co}_2\text{Sn}$. The optical phonons would have a higher frequency and therefore require greater energy to activate in the same order.

3.5. Charge density distribution

The charge density results for the five compounds are shown in Figure 4. Their topology is similar, except for Co_2Si . This may explain why Co_2Si exhibited a much higher Debye temperature than the other compounds. Directional bonding is evident in all the compounds and this is expected to make the compounds exhibit high strength.

4. Conclusions

The site preference of cobalt, the only transition element in the binary half-Heusler alloys of the stoichiometry Co_2X (X= In, Ga, Si, Sn, Sb), is similar to that of the traditional ternary half-Heusler alloys. The two cobalt atoms prefer entering the A and B sites and leaving the C sites unoccupied. All the compounds formed were found to be ferromagnets. The DoS results show that the half metallic character required in materials for spintronic and other important applications can be readily achieved in Co_2Ga and Co_2In with the proper choice of lattice size. The same result can be achieved in Co_2Sb and Co_2Sn . In this case, however, much care is required because the energy gaps in the down band of the materials are narrow. Co_2Si is not an outright half metal, but it is predicted to be an n-type degenerate semiconductor. All the compounds are predicted to exhibit good strength and ductility and this should make the compounds suitable for the manufacturing of engineering components.

Despite the various impressive electronic and mechanical properties in favor of these compounds, Co_2Ga , Co_2Sb , and Co_2Sn are thermodynamically unstable and Co_2In is elastically unstable. The potentials of these

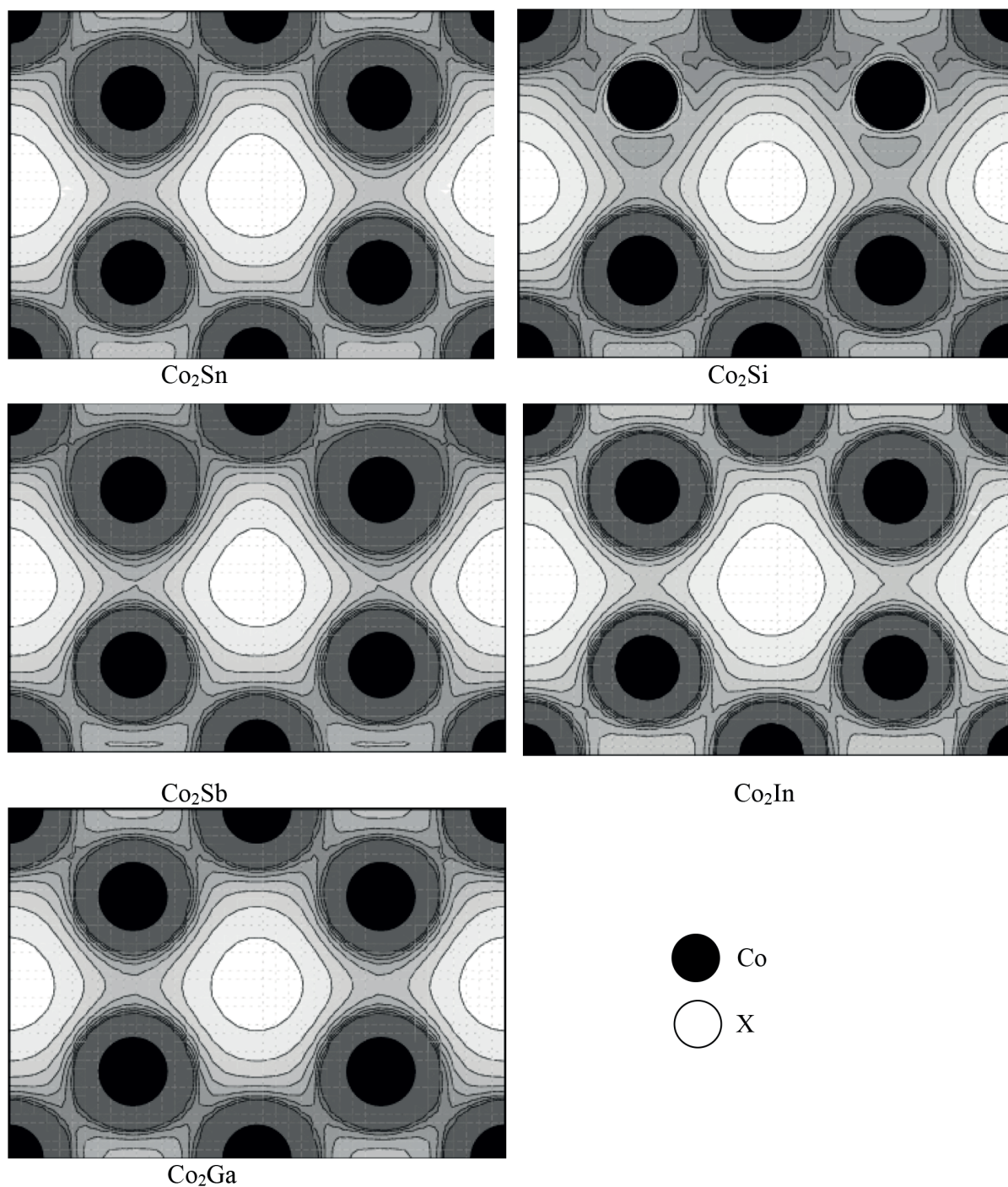


Figure 4. Charge density distribution contour for Co_2Sn (top left), Co_2Si (top right), Co_2Sb (middle left), Co_2In (middle right), and Co_2Ga (bottom left) in the (110) plane.

compounds as advanced materials could perhaps spur the need to find the right approach to synthesize and stabilize them and one such approach could include element addition such as ternary alloying.

Acknowledgments

The author would like to thank Víctor Luaña (Department of Analytical Physics, University of Oviedo) and Alberto Otero-de-la-Roza (University of California, Merced) for making the code to calculate elastic constants with QUANTUM ESPRESSO available free of charge.

References

- [1] Heusler, F. *Verh. Dtsch. Phys. Ges.* **1903**, *5*, 219-223.
- [2] Ziebeck, K. R. A.; Neumann, K. U. In *Magnetic Properties of Metals*; Wijn, H. R. J., Ed. Springer: Berlin, Germany, 2001, pp. 64-414.
- [3] Tobola, J.; Kaprzyk, S.; Pecheur, P. *Phys. Status Solidi B* **2003**, *236*, 531-535.
- [4] Galanakis, I.; Mavropoulos, P. H.; Dederichs, P. H. *J. Phys. D Appl. Phys.* **2006**, *39*, 765-775.
- [5] Poon, S. J. In *Semiconductors and Semimetals: Recent Trends in Thermoelectric Materials Research*; Tritt, T. M., Ed. Academic Press: San Diego, CA, USA, 2000, pp. 37-76.
- [6] Han, C.; Li, Z.; Dou, S. *Chinese Sci. Bull.* **2014**, *59*, 2073-2091.
- [7] Wyckoff, R. W. G. *Crystal Structures*, 2nd ed.; John Wiley: New York, NY, USA, 1963.
- [8] Felser, C.; Hillebrands, B. *J. Phys. D Appl. Phys.* **2009**, *42*, 080301.
- [9] Graf, T.; Felser, C.; Parkin, S. S. P. *Prog. Solid State Chem.* **2011**, *39*, 1-50.
- [10] Deng, Z.; Jin, C. Q.; Liu, Q. Q.; Wang, X. C.; Zhu, J. L.; Feng, S. M.; Chen, L. C.; Yu, R. C.; Arguello, C.; Goko, T. et al. *Nat. Commun.* **2011**, *2*, 1425.
- [11] De Groot, R. A.; Mueller, F. M.; Van Engen, P. G.; Buschow, K. H. J. *Phys. Rev. Lett.* **1983**, *50*, 2024-2027.
- [12] Nanda, B. R. K.; Dasgupta, I. *Comp. Mater. Sci.* **2006**, *36*, 96-101.
- [13] De Groot, R. A. *Physica B* **1991**, *172*, 45-50.
- [14] Casper, F.; Graf T.; Chadov, S.; Balke, B.; Felser, C. *Semicond. Sci. Tech.* **2012**, *27*, 063001.
- [15] Li, J.; Meng, F.; Liu, G.; Chen, X.; Luo, H.; Liu, E.; Guangheng, W. *J. Magn. Magn. Mater.* **2012**, *331*, 82-87.
- [16] Schwarz, K. *J. Phys F Met. Phys.* **1986**, *16*, L211-L215.
- [17] Penicaud, M.; Siberchicot, B.; Sommers, C. B.; Kübler, J. *J. Magn. Magn. Mater.* **1992**, *103*, 212-220.
- [18] Ramirez, A. P. *J. Phys.-Condens. Mat.* **1997**, *9*, 8171-8199.
- [19] Serrate, D.; De Teresa, J. M.; Ibarra, M. R. *J. Phys.-Condens. Mat.* **2007**, *19*, 023201.
- [20] Hohenberg, P.; Kohn, W. *Phys. Rev. B* **1964**, *136*, 864-875.
- [21] Kohn, W.; Sham, L. J. *Phys. Rev. A* **1965**, *140*, 1133-1139.
- [22] Giannozzi, P.; Baroni, S.; Bonini, N.; Calandra, M.; Car, R.; Cavazzoni, C.; Ceresoli, D.; Chiarotti, G. L.; Cococcioni, M.; Dabo, I. et al. *J. Phys.-Condens. Mat.* **2009**, *21*, 395502.
- [23] Perdew, J. P.; Burke, K.; Ernzerhof, M. *Phys. Rev. Lett.* **1996**, *77*, 3865-3868.
- [24] Hendrik, M. J.; James, P. D. *Phys. Rev. B* **1976**, *13*, 5188-5192.
- [25] Catti, M. *Acta Cryst.* **1985**, *41*, 494-500.
- [26] Catti, M. *Acta Cryst.* **1989**, *45*, 20-25.
- [27] Hill, R. *Proc. Phys. Soc. Lond. A* **1952**, *65*, 349-354.
- [28] Blackman, M. *Phil. Mag.* **1951**, *42*, 1441-1442.
- [29] Siethoff, H.; Ahlborn, K. *Phys. Status Solidi B* **1995**, *190*, 179-191.
- [30] Pugh, S. F. *Philos. Mag.* **1954**, *45*, 823-843.